

Outage Performance of a Hybrid DS/FH Spread Spectrum Signal in an ISM band

Hanyu Li, Mubashir Syed, and Yu-Dong Yao[†]

Abstract

This paper develops an analytical model for characterizing the coexistence interference in the unlicensed industrial, scientific and medical (ISM) bands, based on radio frequency measurement results in the 2.4 GHz ISM band. The modeling approach presented here offers a simple methodology for profiling the interference from devices occupying a common spectrum. Outage performance using the interference model is exemplified through the analysis for a hybrid direct-sequence frequency hopping spread spectrum signal. The work presented in this paper looks to provide insight by means of quantitative evaluation of signal outage in a coexistence environment that can be used for engineering design of applications for unlicensed bands as well as function as a tool in the development process for future spectrum management policy models.

Index Terms

Outage probability, ISM band, frequency hopping, direct-sequence spread spectrum.

Hanyu Li and Mubashir Syed are Ph.D. students in the Wireless Information Systems Engineering Laboratory (WISELAB), Department of Electrical & Computer Engineering, Stevens Institute of Technology. Email: {hli5, msyed}@stevens.edu

Yu-Dong Yao is the Director of WISELAB and an Associate Professor in the Department of Electrical & Computer Engineering, Stevens Institute of Technology.

[†]Correspondence to: Yu-Dong Yao, Dept. of Electrical and Computer Engineering, Stevens Institute of Technology, Castle Point on Hudson, Hoboken, NJ 07030. Tel: +1 201 216-5264. Fax: +1 201 216-8246. Email: {yyao}@stevens.edu

Outage Performance of a Hybrid DS/FH Spread Spectrum Signal in an ISM band

I. INTRODUCTION

LICENSING radio frequencies for commercial use has long been the mechanism adopted by regulatory bodies for managing the radio frequency (RF) spectrum. An exclusive license was granted with the intention to protect the licensee's service from interference, but it also allowed the licensee to exclude shared use even when this may result in higher utilization of the allocated spectrum. Justification, in part, for this approach to spectrum management was predicated on technological limitations of old. Although technology has evolved over time and in the process annulled most of these limitations, regulatory spectrum management methodology has failed to keep pace. On the other hand, the industrial, scientific, and medical (ISM) radio bands, originally allocated for non-commercial uses, were later modified to allow for more services,¹ prompting an influx of wireless communications applications (such as wireless local area networks or WLANs, bluetooth etc.) that exploit these bands for license-free operation. This can be seen as an indication of the role that unlicensed bands are set to play in the evolution of wireless services. The traditional philosophy of interference management through licensing and regulatory processes is to protect the licensee from potential sources of interference in the licensed spectrum bands. The unlicensed bands, in contrast, offer no such protection from interference caused by coexisting systems, and resolving interference related problems is a challenge that researchers and system designers have to address.

The dramatic increase in applications associated with the unlicensed bands has brought to the fore two issues that demand synergistic solutions. Motivation for the work presented in this paper is derived from this inference. The first issue is coexistence in unlicensed bands. Successful resolution of this challenge is incumbent on technological innovation. Over time, technological advancement has enabled more efficient and (dynamically) adaptive wireless systems that can allow efficacious

simultaneous frequency reuse. Technologies like smart antennas,^{2,3,4} spread spectrum modulation, software defined radio (SDR)⁵ and cognitive radio⁶ make it feasible for transceivers to dynamically change their frequency, modulation, or power levels to enable more efficient and intelligent spectrum sharing. For example, advances in signal processing technology (e.g., multi-user detection theory⁷) and cooperative networking (e.g., ad hoc networks^{8,9} or grid computing¹⁰) can exploit the fact that there are multiple signal sources sharing the same frequency bands to improve reception gain. The notion of coexistence would in turn drive technological evolution. In light of the progress of technology and evolution of wireless systems, the traditional exclusive-use licensing approach to tackling the interference problem is increasingly being seen as inefficient and restrictive (as also corroborated by the findings of the FCC's Spectrum Policy Task Force¹¹). This is the second issue that needs to be addressed. It is critical that a resolution to this problem abets the evolution of the current 'command and control' approach to spectrum policy into one that promotes greater reliance on market forces for managing how spectrum is used. To this end, characterization of the spectral emissions in the ISM band due to the current range of uncoordinated wireless services that occupy this spectrum, will provide valuable insight.

The sanction for unlicensed use of the ISM band predicates that efficient coexistence is essential for successful operation of systems in this band. This calls for a multifaceted approach to system design, encompassing spectrum occupancy measurements, modeling of coexistence interference, performance evaluation and development of optimum waveforms. A number of studies of spectrum occupancy measurements in the ISM band have already been reported in the literature.^{12,13,14,15} At the Stevens Institute of Technology, an investigative study is being carried out for distributed spectrum occupancy measurements in the 2.4 GHz ISM band.¹⁶ The focus of this paper is on the modeling of interference in the 2.4 GHz ISM band (based on measurement data), and outage performance analysis using the developed interference model. Based on measurement data in typical environments (indoor, outdoor etc.) that provide insight into the spectral emission characteristics and the corresponding sources, we develop an analytical model of the coexistence interference in the 2.4 GHz ISM band. The model exemplifies a simple approach to interference modeling due to uncoordinated sources/technologies sharing a common band of frequencies, given an understanding

of their emission characteristics. It is evident that different statistics are needed to characterize the interfering signals in the ISM band. A simple yet general mathematical approach for interference characterization would serve many a purpose.

Generally, in wireless system engineering, assessment of the effects of interference on system operation is done through the probability of outage, which lends itself well as a statistical measure of radio link performance. In simple terms, outage probability can be defined as the probability that the desired signal-to-interference-plus-noise ratio (SINR) falls below an appropriate threshold that is determined based on system design requirements. The development of mathematical tools for outage analysis has received a lot of attention since the deployment of commercial cellular phone networks.¹⁷ In this paper, we derive the outage probability based on the developed interference model. An analysis based on numerical evaluation of outage and error probabilities is also presented.

The rest of the paper is structured as follows. In the next section, we discuss the 2.4 GHz ISM band occupancy scenarios and describe our approach to characterizing interference for a typical application environment. The signal model that is considered for the analysis in this paper is explained in the subsequent section. Section IV presents mathematical derivations of expressions for capture probabilities; outage and error performance analysis is discussed in Section V. Results of numerical evaluation of the derived performance measures are presented in Section VI. Finally, the work presented in this paper is summarized and conclusions are drawn in Section VII.

II. INTERFERENCE SCENARIOS AND MODELING

It is clear that an increasing number of devices occupy the ISM band frequencies between 2.4 and 2.4835 GHz. As the services that these devices provide are complementary rather than competing, coexistence is seen as the operational norm. Also evident is that these devices, which run the gamut from communications equipment to kitchen aids, are based on different technologies and, therefore, have different emission characteristics. Fig. 1 shows some sample measurements¹⁶ in the 2.4 GHz ISM band that highlight spectrum occupancy by typical devices. From the temporal and spectral emission characteristics, various applications have been identified, including Bluetooth,

IEEE 802.11b WLAN and microwave oven emissions. Additional tone and narrowband emissions have also been observed.

In view of the variations in bandwidth occupancy patterns of coexisting wireless devices and several other factors (such as proximity constraints and application environment etc.), design considerations for effective introduction of additional signal transmissions in the ISM band necessitate that a three-fold approach be employed. The first requirement is to minimize the interference to coexisting services. The second is to quantify the interference from coexisting users. To accurately characterize every interfering signal in the ISM would require quite a few different statistics and would be mathematically unwieldy. However, a simple yet general technique which accounts for the various devices that typically occupy the common spectrum would be useful and also provide an attractive way to address the issue. Finally, building on the above two efforts, effective waveforms that are robust to interference need to be developed. The focus of this paper is to evaluate the impact of interference from coexisting users. Towards this end, we attempt to profile the observed emissions in terms of various representative interference types.

Table I summarizes the interference types of measured ISM band emissions. It is noted that the profiling presented here is derived from the temporal and spectral measurements conducted in a specific office environment with the usual set of devices currently typical in the 2.4 GHz ISM band. The significance of this interference modeling approach is that it showcases a simple and sufficiently accurate methodology for profiling emissions in an unlicensed band that can be used for different interference scenarios. The spectrum occupancy of the ISM band can be characterized in terms of transmission bandwidth and time. Transmissions from devices operating in this band can cover the entire available bandwidth or a part of it. This operational characteristic is considered with respect to the bandwidth of the signal of interest, which is denoted as B and represents the size of a frequency slot within the total available bandwidth. The number of frequency slots that make up the total bandwidth is denoted as N . Thus, the entire ISM band is considered to be divided into N frequency slots, each with bandwidth B . Emissions from different sources also have temporal characteristics such as periodicity and duty cycle. To parameterize these in terms of the signal of interest, a duration of T_h time units is defined. As a result, the periodicity and duty

on-off times of interfering signals can be described with reference to T_h . As listed in the table, the observed emissions are categorized into three broad interference types based on their transmission bandwidth – barrage, partial-band and tone. Barrage type interferers are those whose transmission bandwidth covers the entire signal bandwidth B . Partial-band interference is a generic grouping of interference sources characterized by transmission bandwidth that occupies part of the desired signal bandwidth B . Devices transmitting single frequency impulses are grouped under the tone interference type. Based on the spectral characteristics of the emissions as obtained from measured data, they have been matched to their corresponding device type. Furthermore, to capture the effect of spatial and temporal variation on the emission characteristics of the different interference sources, albeit of the same interference type, it is required that they be classified in terms of additional parameters that would facilitate a more accurate modeling of the interference. Hence, emissions are also parameterized in terms of their received power levels as $Y_{i,j}$, where the first subscript corresponds to the interference type (i.e., $i \in \{1, 2, 3\}$ denoting barrage interference, partial-band interference and tone interference respectively) and the second subscript, j , denotes a specific source of the given interference type. Similarly, the duty cycle of each source is parameterized as $\rho_{i,j}$. Periodicity refers to whether or not an interference type exhibits periodic emission characteristics with respect to the specified reference time duration T_h . It is noted that the various emissions are referenced under the listed interference types based on the bandwidth they occupy with respect to B .

III. SIGNAL MODEL

In order to evaluate the coexistence environment and quantify the interference and its impact, an appropriate signal model has to be adopted. Hybrid spread spectrum (SS), where a direct-sequence (DS) SS modulated signal is frequency hopped according to a specific frequency-hopping (FH) pattern, is an attractive choice. This paper considers such a DS/FH signal for the reasons that it has an inherent capacity to mitigate interference caused to others, by virtue of its low power spectrum density, and interference resistance across multiple bands through FH. Additional interference reduction is provided due to the DS spreading gain. It is noted that in keeping with a

more generalized treatment of the approach presented in this paper and for lucidity of presentation, specifics have been avoided. For instance, explicit details of the signature sequence used for spreading, the frequency hopping pattern and the signal processing aspects of multipath fading have been ignored. Just enough detail is furnished so as to account for the concerned phenomena for our purposes.

For the analysis presented here, a single desired user is considered and all the other transmitting sources occupying the frequency band are taken to be interferers. Noncoherent reception is considered so as to reflect situations where the receiver can acquire time synchronization with the desired signal but it cannot acquire a phase reference. This might be the case because of high levels of interference in the frequency band. Also, modulation schemes that allow for noncoherent reception need to be employed. The modulation scheme of interest here is differential phase shift keying (DPSK). Let us denote the DPSK modulated DS spread signal as $c(t)$, and is given by

$$c(t) = 2\sqrt{2X}b(t)\Psi(t)a(t)\cos(2\pi f_c t + \theta) \quad (1)$$

where f_c is the carrier frequency, X is the power of the transmitted signal, θ is the phase introduced by the DPSK modulator and $\Psi(t)$ is a chip waveform with duration T_c . The data signal, $b(t)$, (which is a differentially encoded version of the information signal) is a sequence of rectangular pulses with amplitude equal to either $+1$ or -1 . The code waveform, $a(t)$ is a periodic sequence of positive and negative rectangular pulses of unit amplitude and duration T_c . The DS-SS signal, $c(t)$, is then frequency-hopped according to the hopping pattern $f(t)$. The transmitted signal takes the form

$$s(t) = \sqrt{2X}b(t)\Psi(t)a(t)\cos\{2\pi[f_c + f(t)]t + \theta + \phi(t)\} \quad (2)$$

where $\phi(t)$ represents the phase waveform introduced by the frequency hopper.

We consider that the propagation channel for the desired signal is characterized by Rayleigh fading with impulse response $h(t)$. Thus, the signal at the input of the receiver is given by

$$\begin{aligned} r(t) &= s(t) \otimes h(t) + y(t) + n(t) \\ &= x(t) + y(t) + n(t) \end{aligned} \quad (3)$$

where \otimes denotes the convolution operation, $y(t)$ denotes the total interference and $n(t)$ is the additive white Gaussian noise (AWGN) with two-sided spectrum density $N_0/2$. The receiver is assumed capable of acquiring the frequency-hopping pattern, signature sequence and time synchronization of the user. The output of the frequency de-hopper in the receiver enters the de-spreader and then the DPSK demodulator.

IV. DERIVATION OF CAPTURE PROBABILITIES

In wireless communications, adequate signal-to-interference-plus-noise ratio (SINR) is essential for successful communications.^{18,19} Therefore, the capture probability, defined as the probability of achieving a SINR sufficient to give satisfactory reception, is an important measure in the evaluation of performance of wireless systems. Mathematically the capture probability P_{cap} is given by

$$\begin{aligned} P_{cap} &= \int_{R_N}^{\infty} p_{\gamma}(\gamma) d\gamma \\ &= \Pr \left\{ \frac{x}{y+n} > R_N \right\} \end{aligned} \quad (4)$$

in which γ is the instantaneous SINR, $p_{\gamma}(\gamma)$ is the probability density function (pdf) of γ , and R_N is a required threshold. The variable γ is a function of x , y and n , with x denoting the desired signal power, y denoting the total interference power and n denoting the noise power. For the derivations presented here, the interfering signals (if any) are considered to be either from one of the above discussed three types (namely, barrage, partial-band or tone interferers), or a combination of these different types. Correspondingly, the capture probabilities are obtained as discussed below.

A. Capture Probabilities without Interference (AWGN Case)

If there is no interferer in the same band while the desired signal is transmitting, AWGN will affect the reception quality. If the AWGN one-sided power spectrum density (psd) is denoted by N_0 , the power of the noise is N_0B . The instantaneous SINR is

$$\gamma = \frac{1.5Gx}{N_0B} \quad (5)$$

in which G is the spreading gain and 1.5 is due to the waveform of spreading sequence. The capture probability is

$$\begin{aligned}
P_{cap} &= \Pr \left\{ \frac{1.5Gx}{N_0B} > R_N \right\} \\
&= \Pr \left\{ x > \frac{N_0BR_N}{1.5G} \right\} \\
&= \int_{\frac{N_0BR_N}{1.5G}}^{\infty} p_x(x) dx \\
&= \exp \left(-\frac{1}{1.5G\Gamma_N} \right)
\end{aligned} \tag{6}$$

in which $p_x(x) = \frac{1}{X} \exp(-\frac{x}{X})$ is the pdf of the Rayleigh faded signal power and $\Gamma_N = \frac{X}{N_0BR_N}$ is the normalized average signal to noise ratio (SNR).

B. Capture Probabilities with Barrage Interference

In this subsection we derive the capture probabilities when the interference is of the first type, i.e., barrage interference. Barrage interferers transmit bandlimited signals at high power. The performance of a spread spectrum signal is the same in the scenario of either AWGN or barrage interferers.²⁰ We begin with analyzing the capture probability under a single barrage interferer, then we will derive the capture probability under multiple barrage interferers.

1) *Capture Probabilities with One Barrage Interferer:* The instantaneous interference power after despreading is denoted as y_1 . Then, the instantaneous SINR is

$$\gamma = \frac{1.5Gx}{y_1 + N_0B} \tag{7}$$

Assuming that the fading statistics of the desired signal and the interferer are independent, the

capture probability is calculated by

$$\begin{aligned}
P_{cap} &= Pr \left\{ \frac{1.5Gx}{y_1 + N_0B} > R_N \right\} \\
&= Pr \left\{ x > \frac{(y_1 + N_0B)R_N}{1.5G} \right\} \\
&= \int_0^\infty p_{y_1}(y_1) \int_{\frac{(y_1 + N_0B)R_N}{1.5G}}^\infty p_x(x) dx dy_1 \\
&= \exp \left(-\frac{1}{1.5G\Gamma_N} \right) \times \frac{1}{1 + \frac{1}{1.5G\Gamma_1}}
\end{aligned} \tag{8}$$

in which $p_{y_1}(y_1)$ is the pdf of the Rayleigh faded interference power and $\Gamma_1 = \frac{X}{Y_1 R_N}$ is the normalized average signal-to-interference ratio (SIR). It is noted that the received interference is considered to have experienced Rayleigh fading. This is a valid assumption considering the environment scenario in which the source of the perceived interference is operating. The capture probability P_{cap} versus SNR Γ_N and SIR Γ_1 is plotted in Figure 2.

2) *Capture Probability with Multiple Barrage Interferers:* If there are I barrage interferers present, and for the j th interferer, denoting its average power as $Y_{1,j}$ and its instantaneous power after despreading as $y_{1,j}$, the instantaneous SINR is

$$\gamma = \frac{1.5Gx}{\sum_{j=1}^I y_{1,j} + N_0B} \tag{9}$$

Assuming that the fading statistics of the desired signal and the interferers are mutually independent,

the capture probability is derived as

$$\begin{aligned}
P_{cap} &= Pr \left\{ \frac{1.5Gx}{\sum_{j=1}^I y_{1,j} + N_0B} > R_N \right\} \\
&= Pr \left\{ x > \frac{(\sum_{j=1}^I y_{1,j} + N_0B)R_N}{1.5G} \right\} \\
&= \int_0^\infty \cdots \int_0^\infty p_{y_{1,1}}(y_{1,1}) \cdots p_{y_{1,I}}(y_{1,I}) \left(\int_{\frac{(\sum_{j=1}^I y_{1,j} + N_0B)R_N}{1.5G}}^\infty p_x(x) \right) dx dy_{1,1} \cdots dy_{1,I} \\
&= \int_0^\infty \cdots \int_0^\infty p_{y_{1,1}}(y_{1,1}) \cdots p_{y_{1,I}}(y_{1,I}) \exp \left(-\frac{(\sum_{j=1}^I y_{1,j} + N_0B)R_N}{1.5GX} \right) dx dy_{1,1} \cdots dy_{1,I} \\
&= \exp \left(-\frac{R_N N_0 B}{1.5GX} \right) \times \prod_{j=1}^I \int_0^\infty \exp \left(-\frac{R_N y_{1,j}}{1.5GX} \right) \frac{1}{Y_{1,j}} \exp \left(-\frac{y_{1,j}}{Y_{1,j}} \right) dy_{1,j} \\
&= \exp \left(-\frac{1}{1.5G\Gamma_N} \right) \times \prod_{j=1}^I \frac{1}{1 + \frac{1}{1.5G\Gamma_{1,j}}}
\end{aligned} \tag{10}$$

in which $\Gamma_{1,j} = \frac{X}{Y_{1,j}R_N}$ is the average SIR accounting for the j th interferer.

C. Capture Probabilities with Partial-band Interference

In this subsection we derive the capture probabilities for the case where the interference occupies part of the hop bandwidth. We begin by considering the received power of a single partial-band interferer and get its corresponding capture probability. We then derive the capture probability with multiple partial-band interferers.

1) *Capture Probability with One Partial-band Interferer:* The received power of a partial-band interferer, with transmit power y_2 , after despreading is given by²⁰

$$\tilde{y}_2 = y_2 \times \frac{1}{B_2} \int_{-B_2}^{B_2} \frac{\sin^2 \left[(\Delta f - f) \frac{2}{B} \right]}{\left[(\Delta f - f) \frac{2}{B} \right]^2} df \tag{11}$$

In the above equation B_2 is the bandwidth of the partial-band interferer, and Δf is the frequency offset between the interferer and signal. Following the same procedure as in the barrage interferer

case, we get the capture probability with one partial-band interferer as

$$P_{cap} = \exp\left(-\frac{1}{1.5G\Gamma_N}\right) \times \frac{1}{1 + \frac{\alpha_2}{1.5G\Gamma_1}} \quad (12)$$

in which α_2 is a coefficient and it can numerically calculated as

$$\alpha_2 = \frac{1}{B_2} \int_{-B_2}^{B_2} \frac{\sin^2\left[(\Delta f - f)\frac{2}{B}\right]}{\left[(\Delta f - f)\frac{2}{B}\right]^2} df \quad (13)$$

2) *Capture Probabilities with Multiple Partial-band Interferers:* If there are J partial-band interferers, with the average transmit power of the j th interferer denoted as $Y_{2,j}$ and its instantaneous power after despreading denoted as $y_{2,j}$, the instantaneous SINR is

$$\gamma = \frac{1.5Gx}{\sum_{j=1}^J y_{2,j} + N_0B} \quad (14)$$

After simplification the capture probability is obtained as

$$P_{cap} = \exp\left(-\frac{1}{1.5G\Gamma_N}\right) \times \prod_{j=1}^J \frac{1}{1 + \frac{\alpha_{2,j}}{1.5G\Gamma_{2,j}}} \quad (15)$$

in which $\Gamma_{2,j} = \frac{X}{Y_{2,j}R_N}$ is the normalized average SIR in the presence of the j th interferer and $\alpha_{2,j}$ is its corresponding coefficient in the form of (13).

D. Capture Probabilities with Tone Interference

In this subsection we consider the capture probabilities in the presence of tone interferers.

1) *Capture Probabilities with a Single Tone Interferer:* The received power of a single tone interferer, with transmit power y_3 , after despreading is found to be²⁰

$$\tilde{y}_3 = y_3 \times \frac{\sin^2\left(\frac{\Delta W}{2B}\right)}{2\left(\frac{\Delta W}{2B}\right)^2} \left(1 + \frac{\cos\left(2\Delta\phi + G\frac{\Delta W}{B}\right) \sin\left(G\frac{\Delta W}{B}\right)}{G \sin\left(\frac{\Delta W}{B}\right)}\right) \quad (16)$$

In which ΔW and $\Delta\phi$ are the frequency and phase offset between the interferer and the signal. Following the same procedure as in the barrage interferer case we get the capture probability under

a lone tone interferer as

$$P_{cap} = \exp\left(-\frac{1}{1.5G\Gamma_N}\right) \times \frac{\alpha_3}{1 + \frac{1}{1.5G\Gamma_1}} \quad (17)$$

in which α_3 is a coefficient and

$$\alpha_3 = \frac{\sin^2\left(\frac{\Delta W}{2B}\right)}{2\left(\frac{\Delta W}{2B}\right)^2} \left(1 + \frac{\cos\left(2\Delta\phi + G\frac{\Delta W}{B}\right) \sin\left(G\frac{\Delta W}{B}\right)}{G \sin\left(\frac{\Delta W}{B}\right)}\right) \quad (18)$$

2) *Capture Probability with Multiple Tone Interferers:* Lets consider that there are K tone interferers. For interferer j , the average transmit power is denoted as $Y_{3,j}$ and the instantaneous power after despreading is denoted as $y_{3,j}$. Then, the instantaneous SINR is

$$\gamma = \frac{1.5Gx}{\sum_{j=1}^K y_{3,j} + N_0B} \quad (19)$$

And the capture probability is

$$P_{cap} = \exp\left(-\frac{1}{1.5G\Gamma_N}\right) \times \prod_{j=1}^K \frac{1}{1 + \frac{\alpha_{3,j}}{1.5G\Gamma_{3,j}}} \quad (20)$$

in which $\Gamma_{3,j} = \frac{X}{Y_{3,j}R_N}$ is the normalized average SIR in the presence of the j th interferer and $\alpha_{3,j}$ is its corresponding coefficient.

E. Capture Probability with Different Interference Types

There are three types of interferers. Our derivations above are based on the assumption that only one type of interferer is present at a given time. Assuming there are K_1 barrage interferers (each with average transmit power $Y_{1,j}$), K_2 partial-band interferers (each with average transmit power $Y_{2,j}$) and K_3 tone interferers (each with average transmit power $Y_{3,j}$) at the same time, the instantaneous SINR is

$$\gamma = \frac{1.5Gx}{\sum_{i=1}^3 \sum_{j=1}^{K_i} y_{i,j} + N_0B} \quad (21)$$

If we assume that the fading statistics of the desired signal and the interferers are mutually independent, the capture probability is calculated as

$$P_{cap} = Pr \left\{ \frac{1.5Gx}{\sum_{i=1}^3 \sum_{j=1}^{K_i} y_{i,j} + N_0B} > R_N \right\} \quad (22)$$

$$= \exp \left(-\frac{1}{1.5G\Gamma_N} \right) \times \prod_{i=1}^3 \prod_{j=1}^{K_i} \frac{1}{1 + \frac{\alpha_{i,j}}{1.5G\Gamma_{i,j}}}$$

in which $\Gamma_{i,j} = \frac{X}{Y_{i,j}R_N}$ is the normalized average SIR corresponding to interferer j of the i th type. $\alpha_{i,j}$ is its coefficient; $\alpha_{1,j} = 1$, $\alpha_{2,j}$ and $\alpha_{3,j}$ can be found by (13) and (18).

The above result (22) is derived based on a specific set values of interferer parameters $\alpha_{i,j}$. If the $\alpha_{i,j}$ is a random variable, the average capture probability becomes

$$P_{cap} = \int \int \dots \int \exp \left(-\frac{1}{1.5G\Gamma_N} \right) \prod_{i=1}^3 \prod_{j=1}^{K_i} \frac{1}{1 + \frac{\alpha_{i,j}}{1.5G\Gamma_{i,j}}} \times [p_{\alpha_{1,1}}(\alpha_{1,1})p_{\alpha_{1,2}}(\alpha_{1,2})\dots p_{\alpha_{1,K_1}}(\alpha_{1,K_1})\dots p_{\alpha_{3,K_3}}(\alpha_{3,K_3})d\alpha_{1,1}d\alpha_{1,2}\dots d\alpha_{1,K_1}\dots d\alpha_{3,K_3}]$$

$$= \exp \left(-\frac{1}{1.5G\Gamma_N} \right) \left[\prod_{i=1}^3 \prod_{j=1}^{K_i} \int \frac{1}{1 + \frac{\alpha_{i,j}}{1.5G\Gamma_{i,j}}} p_{\alpha_{i,j}}(\alpha_{i,j})d\alpha_{i,j} \right] \quad (23)$$

where $p_{\alpha_{i,j}}(\alpha_{i,j})$ is the pdf of $\alpha_{i,j}$.

V. OUTAGE AND ERROR PERFORMANCE OF A DS/FH SIGNAL

Successful signal transmission in a wireless environment dictates that the desired signal be received with adequate strength and signal-to-interference-plus-noise ratio in the presence of interfering emissions from other sources. Outage probability and packet error rate are two widely used metrics for performance analysis. In this paper, we are interested in quantifying the performance of a DS/FH signal operating in an unlicensed band. Therefore, utilizing the the closed-form capture probabilities of a DS/FH signal derived in the previous section, we derive its outage probability in this section. Packet error rate of a DS/FH signal is also derived considering the use of forward error correction (FEC) coding.

A. Outage Probability

Considering that the duty cycle of an interferer is $\rho_{i,j}$, the probability that the interferer is present in a certain channel (slot) is $\frac{\rho_{i,j}}{N}$, in which N is the total number of available channels. Let the total number of interferers of the three interference types be denoted as K_1 , K_2 , and K_3 respectively. The outage probability of a DS/FH signal is obtained as

$$\begin{aligned}
 P_{out} &= 1 - P_{cap}[All\ Interferers] \\
 &= 1 - \sum_{l_{1,1}=0}^1 \sum_{l_{1,2}=0}^1 \cdots \sum_{l_{1,K_1}=0}^1 \cdots \sum_{l_{3,K_3}=0}^1 \left(\exp\left(-\frac{1}{1.5G\Gamma_N}\right) \prod_{i=1}^3 \prod_{j=1}^{K_i} \left(\int \frac{\alpha_{i,j}}{1 + \frac{1}{1.5G\Gamma_{i,j}}} p_{\alpha_{i,j}}(\alpha_{i,j}) d\alpha_{i,j} \right)^{l_{i,j}} \right) \\
 &\quad \times \left(\prod_{i=1}^3 \prod_{j=1}^{K_i} \left(\frac{\rho_{i,j}}{N} \right)^{l_{i,j}} \left(1 - \frac{\rho_{i,j}}{N} \right)^{1-l_{i,j}} \right)
 \end{aligned} \tag{24}$$

in which $l_{i,j} = \{0, 1\}$ indicates the absence or presence of the j th interferer of type i . If all the interferers of a given type have the same transmitting power, duty cycle, and coefficients, (24) reduces to

$$P_{out} = 1 - \sum_{k_1=1}^{K_1} \sum_{k_2=1}^{K_2} \sum_{k_3=1}^{K_3} \left(\exp\left(-\frac{1}{1.5G\Gamma_N}\right) \prod_{i=1}^3 \left(\frac{1}{1 + \frac{\alpha_i}{1.5G\Gamma_i}} \right)^{k_i} \right) p(k_1)p(k_2)p(k_3) \tag{25}$$

where

$$\begin{aligned}
 p(k_1) &= \binom{K_1}{k_1} \left(\frac{\rho_1}{N} \right)^{k_1} \left(1 - \frac{\rho_1}{N} \right)^{(K_1-k_1)} \\
 p(k_2) &= \binom{K_2}{k_2} \left(\frac{\rho_2}{N} \right)^{k_2} \left(1 - \frac{\rho_2}{N} \right)^{(K_2-k_2)} \\
 p(k_3) &= \binom{K_3}{k_3} \left(\frac{\rho_3}{N} \right)^{k_3} \left(1 - \frac{\rho_3}{N} \right)^{(K_3-k_3)}
 \end{aligned} \tag{26}$$

B. Packet Error Probability

Reed-Solomon (RS) code is an effective FEC coding scheme used in packet transmissions. If the code length is L and its symbol error correction capability is R_C , the packet error probability is

$$P_e = 1 - \sum_{i=0}^{R_C} \binom{L}{i} P_{out}^i (1 - P_{out})^{L-i} \tag{27}$$

in which the outage probability P_{out} can be calculated using the results in (24) or (25).

VI. NUMERICAL ANALYSIS

This section presents numerical results based on the derivations in Sections IV and V. For the performance evaluation presented here, the desired signal is considered to be a DS/FH signal with spreading gain $G = 50$ and occupying a 1 MHz bandwidth (i.e., $B = 1$ MHz), which is reflective of a typical transmission bandwidth of a frequency hopping signal. The propagation of signals from the desired transmitter as well as interfering sources to the receiver in a typical environment where such devices as those that operate in the ISM band used, is well modeled through Rayleigh fading. It is reasonable to assume that the transmissions from the various sources are independent of each other. Therefore, all the signals at the receiver are considered to have undergone mutually independent Rayleigh fading.

Fig. 2 shows the capture probability of a DS/FH signal in the presence of barrage interference. Here we use barrage interference to model interfering emissions that occupy a bandwidth much larger than that occupied by the desired signal during a given hop duration. Capture probability of the desired signal, evaluated using (8), is plotted against normalized SNR and normalized SIR for four scenarios, with different number of interferers. An SINR threshold of 0 dB is assumed. This can be understood as indicative of the upper performance bound since a 0 dB threshold implies that the signal can be successfully detected even when its received power is only equal to the total interference plus noise power. In Fig. 2(a) one barrage interferer is considered in the evaluation. Sub-plots (b), (c) and (d) in Fig. 2 correspond to the cases with 3, 10 and 100 interferers respectively. The variation in the transmitted powers of different sources of interference, and that of the desired signal, can be understood in terms of different SIR values; the effect this has on the capture probability of the DS/FH signal is seen in the plots. The plots also show how SNR affects the capture probability. It is evident that the capture probability can be limited by either SNR or SIR.

Fig. 3 illustrates the capture probability under a combination of interference types. In the evaluations, multiple interferers from each interference type are considered to be transmitting in the shared frequency band – five barrage interferers, five partial-band interferers and eight tone interferers. To analyze the effect of temporal and spatial dynamics of the interferers (in terms of power levels and

emission activity) on receiver capture, a wide range of SIR values are plotted against the capture probability, for a fixed SNR value of 0 dB. The number of channels available for the DS/FH signal to hop is denoted as N . A higher value of N means a larger shared bandwidth. For a given number of interferers operating in the frequency band, this translates into increased diversity in terms of frequency channels utilized for transmission. This, in turn, would lead to improved performance. Three different values of N are considered here ($N = \{10, 40, 80\}$). The duty cycle, ρ , characterizes the on-off operation of an interferer. For the evaluation presented here, two scenarios are considered, namely, ‘low ρ ’ (with the values $\rho_1 = \rho_2 = \rho_3 = 0.2$ for the three types of interferers) and ‘high ρ ’ ($\rho_1 = \rho_2 = \rho_3 = 1$). Two sets of curves are plotted in Fig. 3, corresponding to ‘low ρ ’ and ‘high ρ ’, for the three values of N . The bandwidth B_2 and frequency offset Δf of the partial-band interferer are chosen as zero and $B/2$ respectively. The two parameters, ΔW and $\Delta\phi$, characterizing frequency and phase offset of tone interferers with respect to the desired signal, are both set to zero. These values imply the case where the interferers have the most impact on the desired signal.

The outage probability and packet error probability of a DS/FH signal under multiple interferers are plotted in Fig. 4 and Fig. 5 respectively. Outage probability in a hop duration is evaluated using Eq. (24). The number of hopping channels is assumed to be 80 (i.e., $N = 80$) and the interference bandwidth and offsets are set to the same values as for Fig. 3. Outage probability is plotted against a range of SNR values for three different SIR scenarios (-20 dB, -10 dB and 0 dB) and two set of values for the number of interferers – (i) 12 interferers (3 barrage, 3 partial-band and 6 tone interferers) (ii) 50 interferers (15 barrage, 15 partial-band and 20 tone interferers). The duty cycle of the interferers belonging to the same interference type is assumed to be the same. This considers the scenario where multiple transmitting devices belonging to a given type of system and conforming to the same set of protocols are operating. The chosen values are $\rho_1 = 0.5$, $\rho_2 = 0.7$ and $\rho_3 = 0.9$ for the three corresponding interference types. It is observed from the plots that at high SIR and SNR values, the actual number of interferers does not have a very strong bearing on the outage probability. At lower SIR values, however, even with high SNR the difference in the outage probability of a DS/FH signal in the presence of a few interferers and many interferers is more pronounced. This suggests that a fewer number of interferers transmitting at high power levels

would be more damaging to the desired signal than numerous interferers emitting at low power levels. In Fig. 5, we have plotted the packet error probability against SNR for fixed SIR values. The packet error probability has been evaluated using Eq. (27). All the parameters related to interferers are the same as in Fig. 3. The FEC code for the packet is assumed to be a Reed-Solomon code with parameters values $L = 16$ and $R_C = 4$. Therefore, the RS code can correct up to 4 symbol errors. For the given code length and coding scheme, it is seen that to achieve an adequate packet error rate (of the order of 10^{-5}), a normalized SNR of about -2 dB is required with a normalized SIR of 0 dB.

VII. CONCLUSION

In this paper, we have investigated the issue of coexistence interference in unlicensed bands. Motivation for the work presented here stems from the widespread use of the 2.4 GHz ISM band for varied services and the growing realization of the inadequacy of the licensing methodology for spectrum management that is currently in place. The paradigm for operation in an unlicensed band is to minimize the interference caused to other users in the band and to avoid and suppress the interference from coexisting devices. Towards this, interference modeling is often used to get a better understanding of the operating environment and is central to the evaluation of radio link performance. Based on measurement studies in the 2.4 GHz ISM band, an analytical interference model has been developed in this paper. The modeling approach adopted involves profiling the observed emissions under different interference types based on their spectral characteristics. This offers the convenience of statistically characterizing interference with satisfactory accuracy and in terms of generic models rather than requiring that each source of interference be specifically defined to reflect its temporal and spectral emission characteristics. Such an approach to interference modeling can be utilized in the development of interference management strategies for unlicensed bands. The effect of coexistence interference in the 2.4 GHz ISM band on the performance of a hybrid DS/FH signal, in terms of outage probability and packet error probability, has also been evaluated in this paper. For this, the capture probabilities of a Rayleigh faded signal in the presence of interfering transmissions from coexisting sources were derived; considering both scenarios, when

interferers of the same type are present as well as the one with a combination of the different interference types. Expressions for the outage probability and the packet error probability (in terms of the capture probabilities) were then derived. Results of numerical evaluation of the derived performance measures have been presented. This study is part of our ongoing effort to develop an analytical framework for interference modeling and performance evaluation in the unlicensed band, as it is seen an invaluable tool for interference management.

REFERENCES

1. Code of federal regulations (CFR) title 47: Telecommunication — part 15: Radio frequency devices, October 2004.
2. J. H. Winters. Smart antennas for wireless systems. *IEEE Personal Communications Magazine*, 5:23–27, February 1998.
3. Joseph Liberti and Theodore S. Rappaport. *Smart Antennas for Wireless Communications: IS-95 and Third Generation CDMA Applications*. Prentice Hall PTR, NJ, April 1999.
4. A. Alexiou and M. Haardt. Smart antenna technologies for future wireless systems: trends and challenges. *IEEE Communications Magazine*, 42(9):90 – 97, September 2004.
5. Jeffrey H. Reed. *Software Radio: A Modern Approach to Radio Engineering*. Prentice Hall PTR, NJ, May 2002.
6. Simon Haykin. Cognitive radio: Brain – empowered wireless communications. 23(2), 2005.
7. S. Moshavi. Multi-user detection for DS-CDMA communications. *IEEE Communications Magazine*, 34(10):124–136, October 1996.
8. Charles E. Perkins, editor. *Ad hoc Networking*. Addison-Wesley, Boston, MA, 2001.
9. Stefano Basagni, Marco Conti, Silvia Giordano, and Ivan Stojmenović, editors. *Mobile Ad hoc Networking*. Wiley-IEEE Press, Hoboken, NJ, 2004.
10. F. Darema. Grid computing and beyond: The context of dynamic data driven applications systems. *Proceedings of the IEEE*, 93(3):692–697, March 2005.
11. Spectrum policy task force report, November 2002.
12. P. B. Kenington and D. W. Bennett. Field measurements study into the potential effects of ISM emissions on cellular radio equipment. *IEE Proceedings – Science, Measurement and Technology*, 144(3):134–140, May 1997.
13. C. -C. Huang and R. Khayata. Delay spreads and channel dynamics measurements at ISM bands. In *Proc. IEEE International Conference on Communications – Discovering a New World of Communications (SUPERCOMM/ICC 92)*, volume 3.
14. K. Giannopoulou, A. Katsareli, D. Dres, D. Vouyioukas, and P. Constantinou. Measurements for 2.4 ghz spread spectrum system in modern office buildings. In *Proc. 10th Mediterranean Electrotechnical Conference (MELECON 2000)*, volume 1.

15. M. Biggs, A. Henley, and T. Clarkson. Occupancy analysis of the 2.4 GHz ISM band. *IEE Proceedings – Communications*, 151(5):481 – 488, October 2004.
16. Theodoros Kamakaris and Jason Evans. Distributed spectrum measurements. Proc. Twenty-fourth Annual Joint Conference of the IEEE Computer and Communications Societies (INFOCOM 2005), March 2005.
17. A. Annamalai, C. Tellambura, and V. K. Bhargava. Simple and accurate methods for outage analysis in cellular mobile radio systems — a unified approach. *IEEE Transactions on Communications*, 49(2):303 – 316, February 2001.
18. Y. D. Yao and A. U. H. Sheikh. Investigations into cochannel interference in microcellular mobile radio systems. *IEEE Trans. Veh. Tech.*, 41(2):114–123, May 1992.
19. Y. D. Yao and A. U. H. Sheikh. Outage probability analysis for microcell mobile radio systems with cochannel interferers in rician/rayleigh fading environment. *Electronic letters*, 26(13):864–866, June 1990.
20. R. L. Peterson, R. E. Ziemer, and D. E. Borth. *Introduction to Spread Spectrum Communications*. Prentice Hall, NJ, 1995.

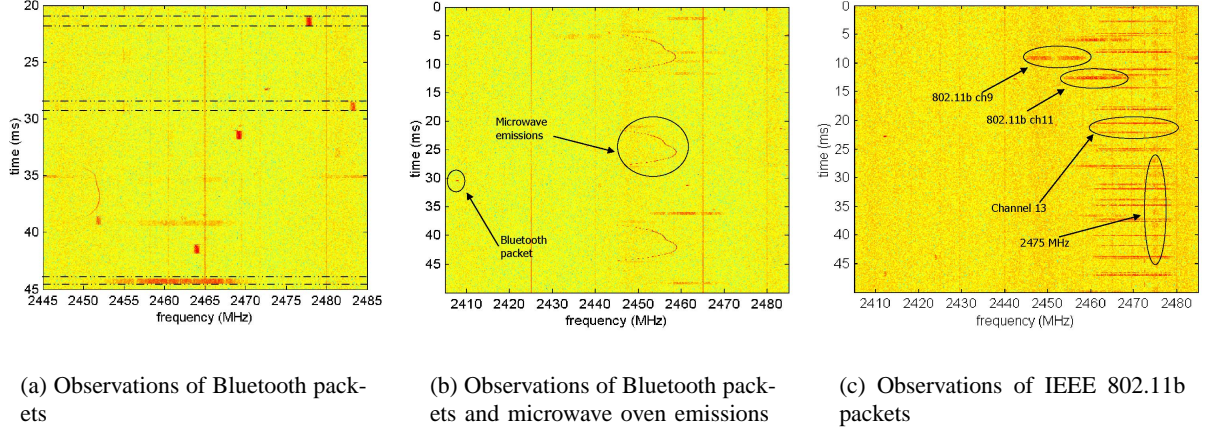
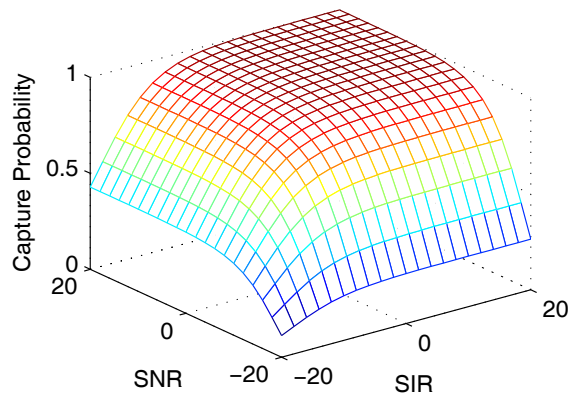


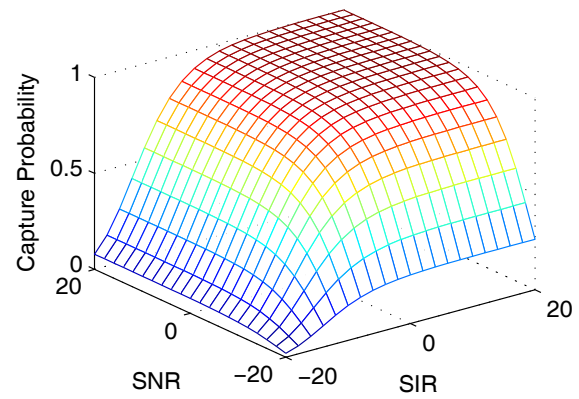
Fig. 1. ISM band spectral emission measurement.¹⁶

TABLE I
2.4 GHz ISM BAND INTERFERENCE CHARACTERISTICS BASED ON MEASUREMENTS.

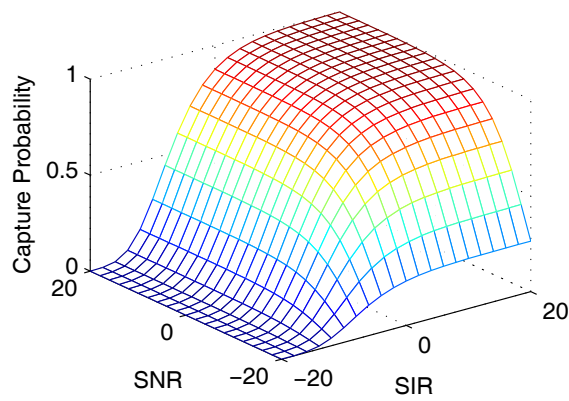
Emissions	Interference Type	Power Level	Duty Cycle	Periodicity	Bandwidth
802.11b packets	Barrage	$Y_{1,j}$	$\rho_{1,j}$	No	$\gg B$
Microwave oven	Barrage	$Y_{1,j}$	$\rho_{1,j}$	Yes	$\gg B$
Bluetooth packets	Partial-band	$Y_{2,j}$	$\rho_{2,j}$	No	$\approx B$
Others	Tone	$Y_{3,j}$	$\rho_{3,j}$	Yes	$\ll B$



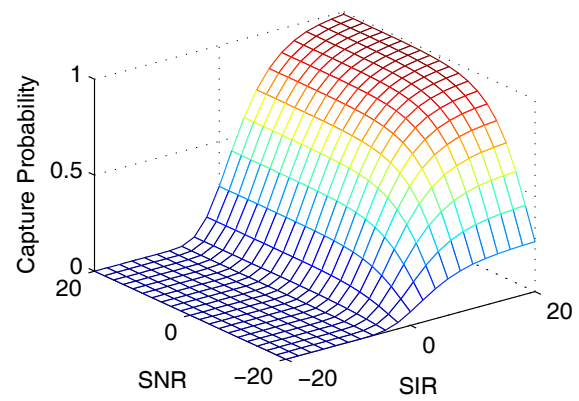
(a)



(b)



(c)



(d)

Fig. 2. Capture probability in the presence of barrage interference. (a) 1 interferer (b) 3 interferers (c) 10 interferers (d) 100 interferers. SIR and SNR are expressed in dB.

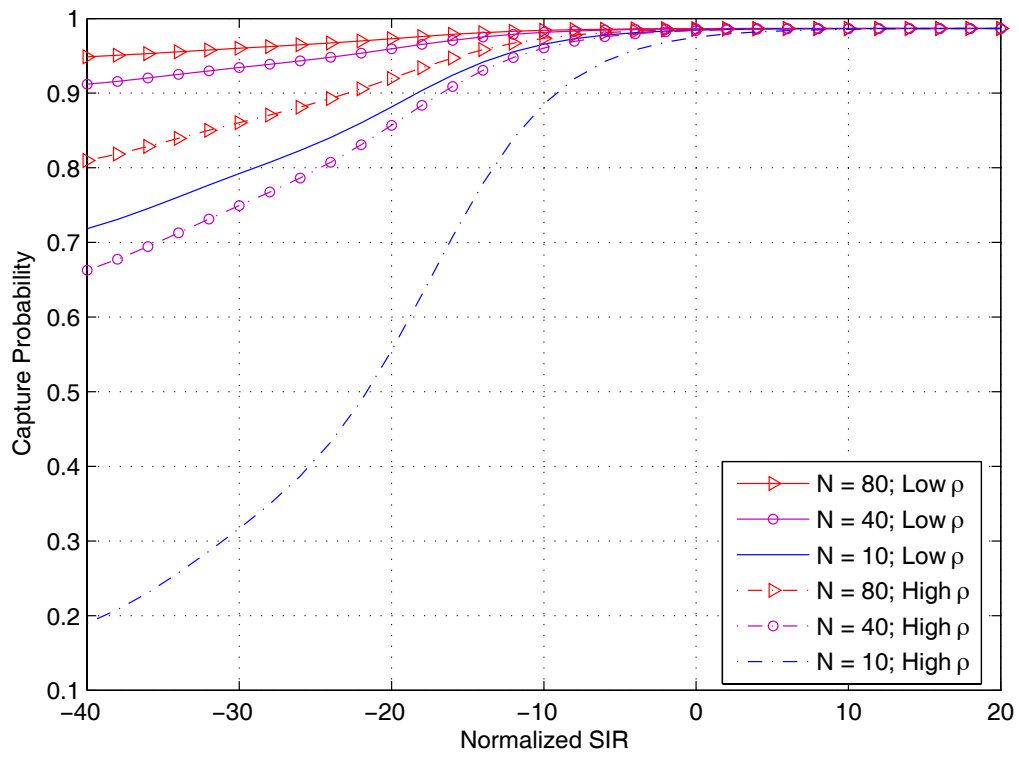


Fig. 3. Capture probability of a DS/FH signal. 5 barrage interferers, 5 partial-band interferers and 8 tone interferers. SIR is expressed in dB.

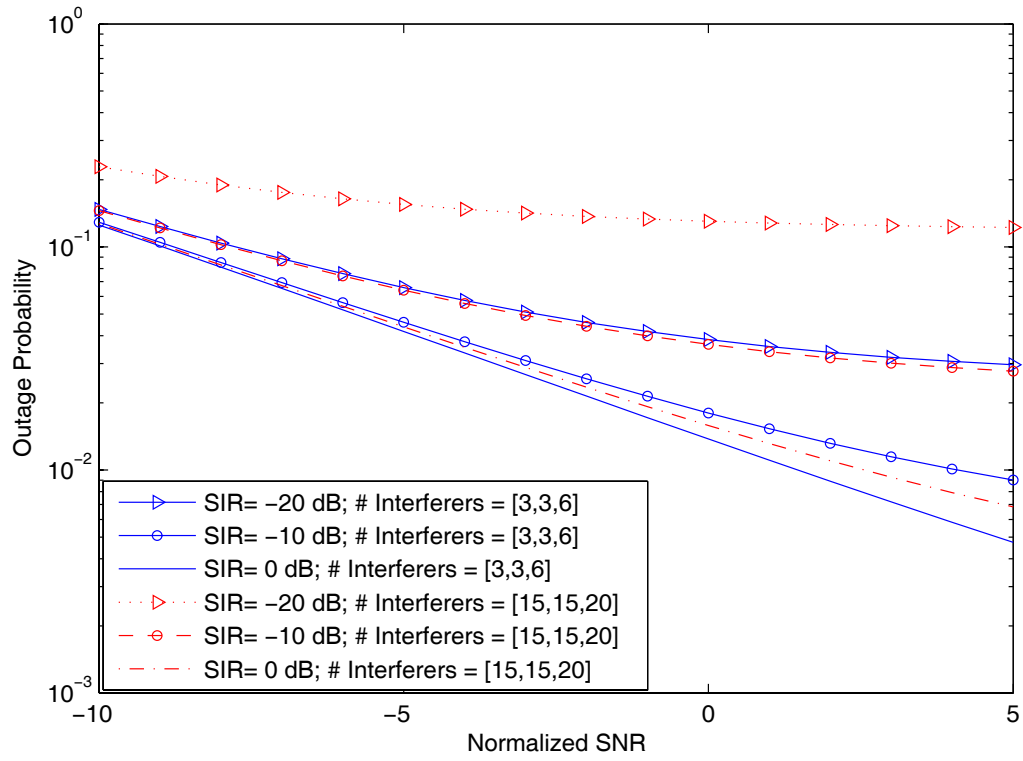


Fig. 4. Outage probability of a DS/FH signal with multiple interferers. $\rho_1 = 0.5$, $\rho_2 = 0.7$ and $\rho_3 = 0.9$. SIR and SNR are expressed in dB.

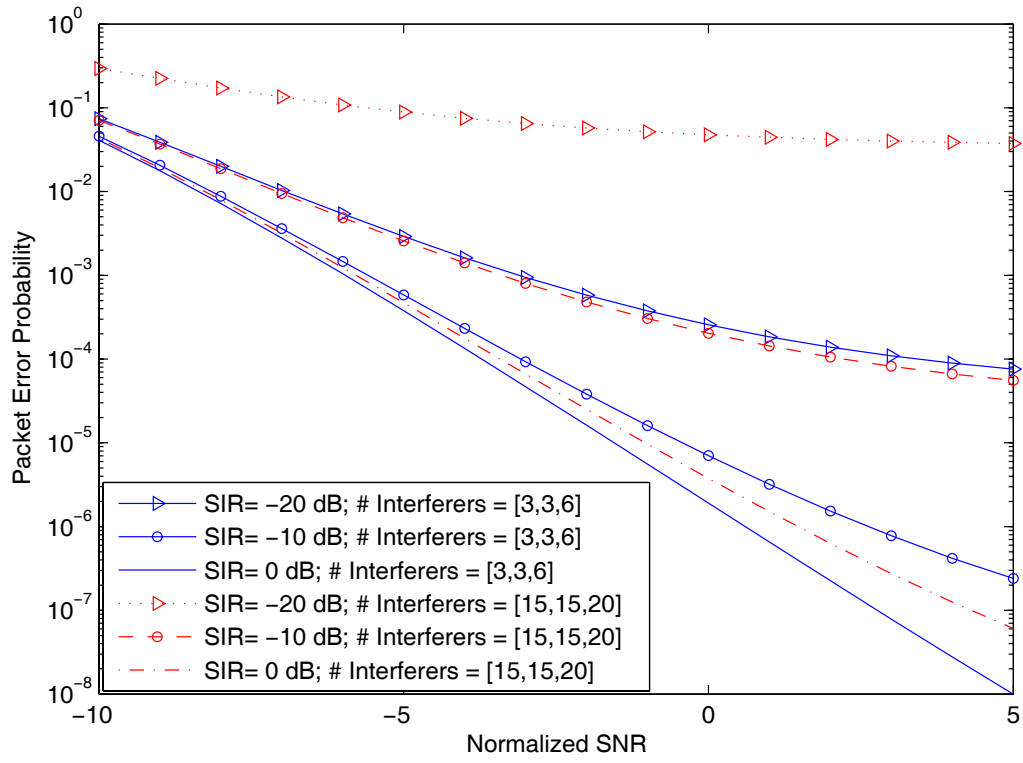


Fig. 5. Packet error probability of a DS/FH signal with multiple interferers. $\rho_1 = 0.5$, $\rho_2 = 0.7$ and $\rho_3 = 0.9$. (16,8) RS code is used. SIR and SNR are expressed in dB.